Supporting Information

NIR squaraine dyes for the dual colorimetric and fluorescent determination of Fe^{3+}, Cu^{2+} and Hg^{2+} ions

Huifang Li[1], Yiru Tang[1], Kunrong Shen, Ji Lu, Zhijie Zhang, Dong Yi, Na Hao, Qiang Fu, Zi Ye, Jun Wei, Jun Wang, Xianchao Pan, Siping Wei*, Lin Yang*

Green Pharmaceutical Technology Key Laboratory of Luzhou City, Central Nervous System Drug Key Laboratory of Sichuan Province, School of Pharmacy, Southwest Medical University, Luzhou 646000, PR China

* Corresponding author. E-mail addresses: swei1225@swmu.edu.cn (Siping Wei), yanglinyjl@swmu.edu.cn (Lin Yang).

[1] These authors contributed equally.

Contents

Table S1 Summary of organic materials-based colorimetric and fluorimetric sensors for metal ions detection.

Sensor No.	Sensing ions	$\lambda_{ex}/\lambda_{em}$[nm]	LOD	Response time	Core Structure	Sensor type	Ref.
1	Fe^{3+}	520/582	41 nM	10 min	Rhodamine	Turn-on	[1]
2	Fe^{3+}	390/440	75 nM	1 min	Pyrene	Turn-on	[2]
3	Fe^{3+}, Hg^{2+}	384/438	98 nM 27.2 nM	-	Rhodamine naphthalimide	Turn-on	[3]
4	Fe^{3+}	448/488 ,561	4.3 μM	2 min	Coumarin	Turn-on	[4]
5	Fe^{3+}	530/551	9.2 nm	6 min	Rhodamine	On-off	[5]
6	Cu^{2+}	420/408	10 μM	-	Naphthol	Turn-off Colorimetric response	[6]
7	Cu^{2+}	680/700	29 nM	15 min	2-picolinic ester	Turn-on 25-fold fluorescence enhancement	[7]
8	Cu^{2+}	435/532	52 μM	60 min	Naphthalene imide	Turn-on	[8]
9	Cu^{2+}	426/590	0.2 μM	20 min	Rhodamine	Turn-on	[9]
10	Cu^{2+}	510/596	42.3 nM	3 min	Coumarin	Turn-on	[10]
11	Hg^{2+}	530/580	1 ppb	5 min	Rhodamine B	On-off	[11]
12	Hg^{2+}	540/575	70 nM	30 min	Schiff-base	Turn-on	[12]
13	Hg^{2+}	530/582	0.18 μM	5 s	Rhodamine	Turn-on	[13]
14	Hg^{2+}	370/420 370/530	49 nM	150 min 50 min	8-amino BODIPY	Turn-on	[14]
15	Fe^{3+} Cu^{2+} Hg^{2+}	663/686	Fe^{3+}:14.17 μM Cu^{2+}:6.06 μM	A few seconds	Squaraine	Turn-off	This work

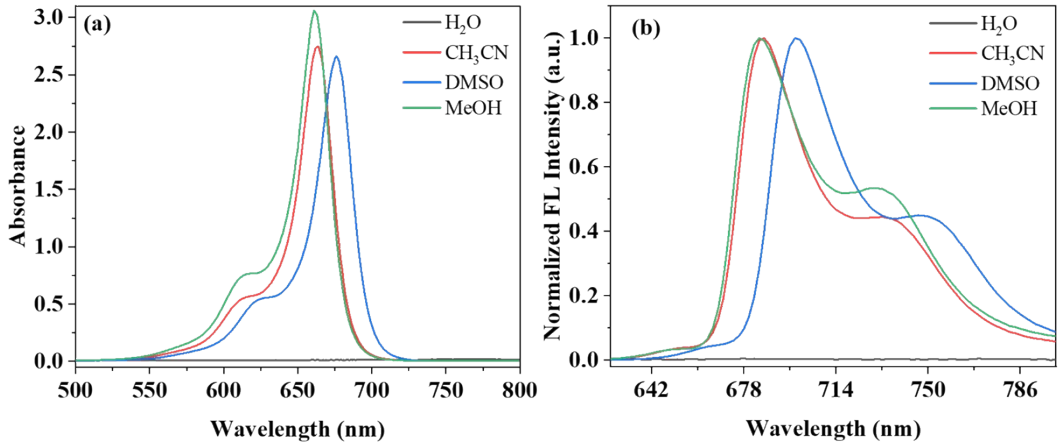

Figure S1 (a) UV-vis absorption spectra and (b) fluorescence emission spectra of BBSQ (10 μM) with different solvents.

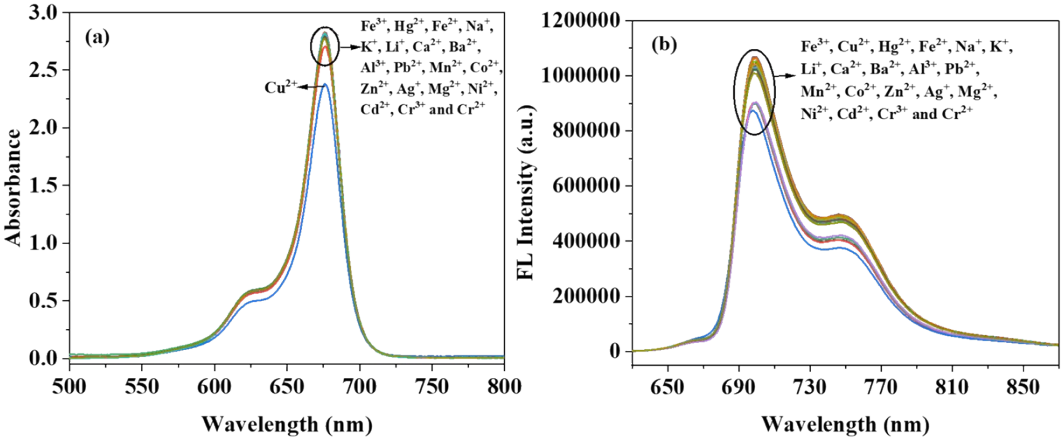

Figure S2 (a) UV-vis absorption spectra and (b) fluorescence emission spectra of BBSQ (DMSO, 10 μM) with different metal ions (20 equiv.).

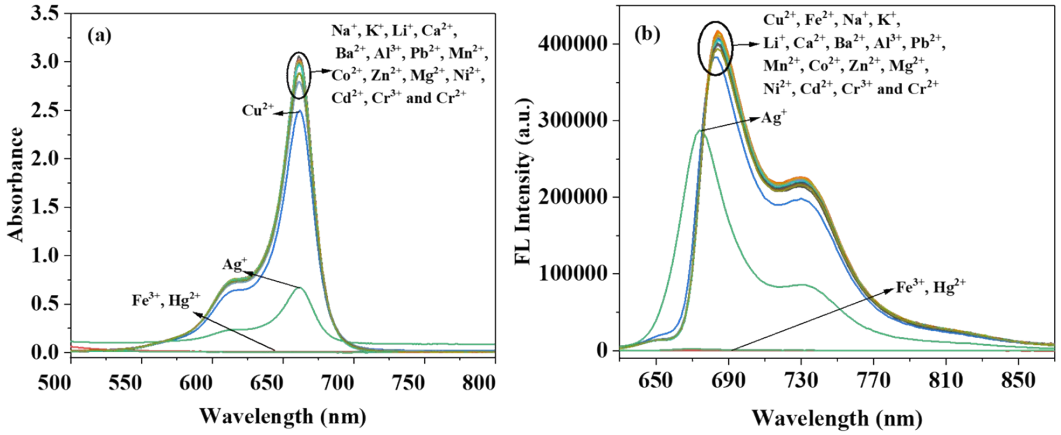

Figure S3 (a) UV-vis absorption spectra and (b) fluorescence emission spectra of BBSQ (MeOH, 10 μM) with different metal ions (20 equiv.).

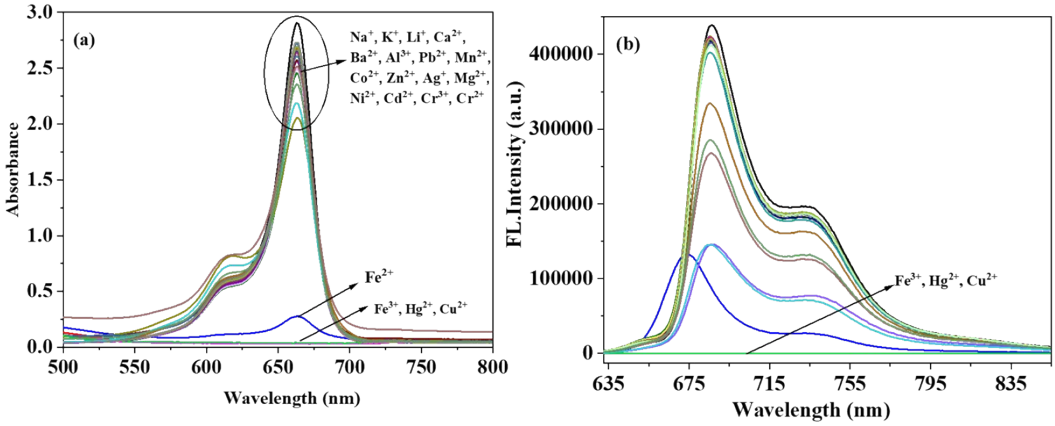

Figure S4 (a) UV-vis absorption spectra and (b) fluorescence emission spectra of BBSQ (CH_3CN, 10 μM) with different metal ions (20 equiv.).

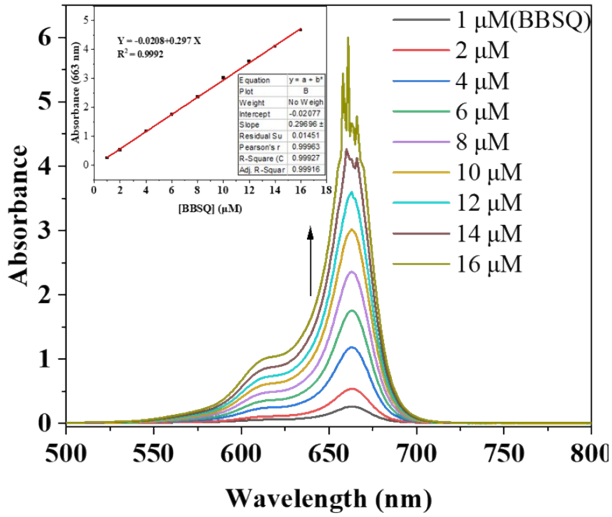

Figure S5 UV-vis absorption spectra of BBSQ (CH_3CN) with different concentration; inset: the linear correlation curve of absorbance at 663 nm with increasing BBSQ concentration.

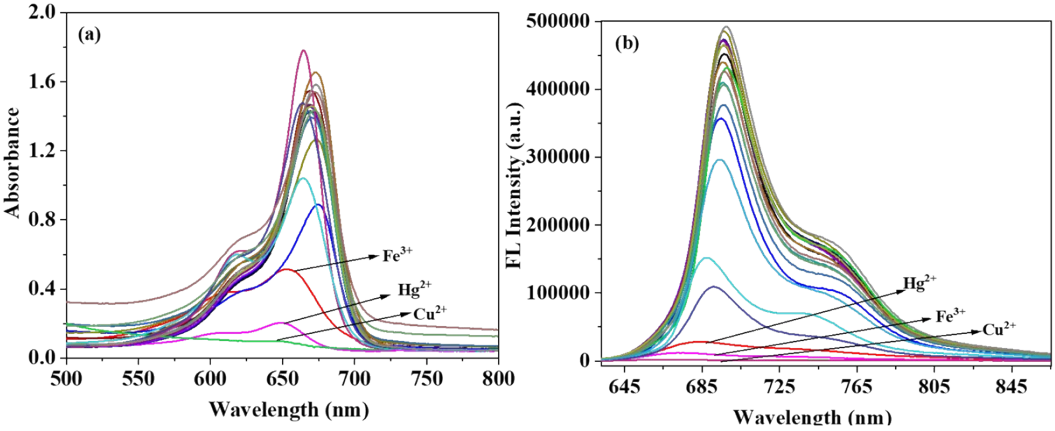

Figure S6 (a) UV-vis absorption spectra and (b) fluorescence emission spectra of BBSQ-S (CH_3CN, 10 μM) with different metal ions (20 equiv.).

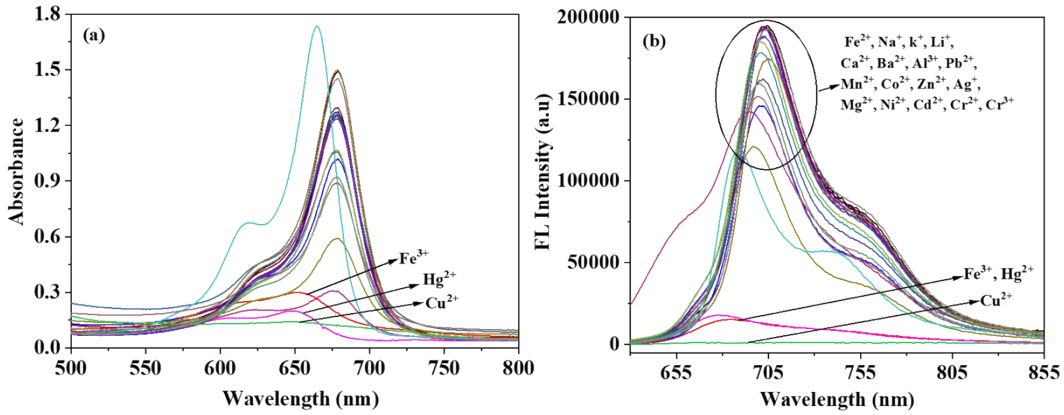

Figure S7 (a) UV-vis absorption spectra and (b) fluorescence emission spectra of BBSQ-SS (CH_3CN, 10 μM) with different metal ions (20 equiv.).

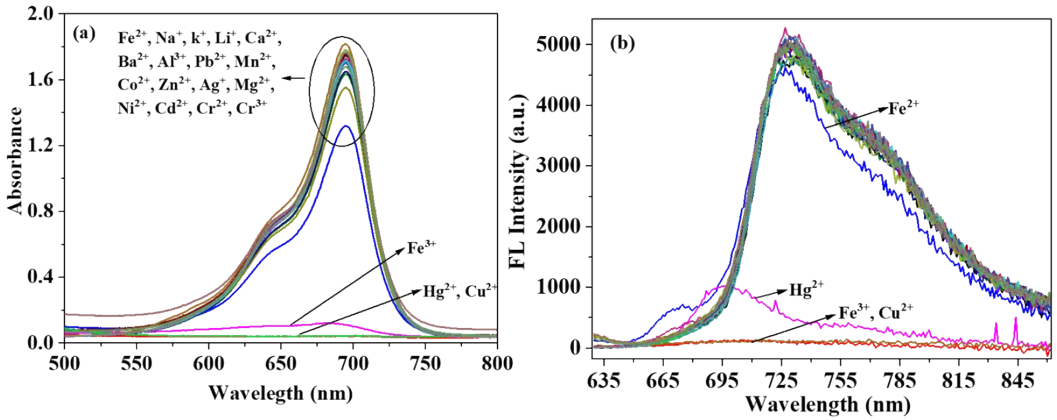

Figure S8 (a) UV-vis absorption spectra and (b) fluorescence emission spectra of BBSQ-NEt (CH_3CN, 10 μM) with different metal ions (20 equiv.).

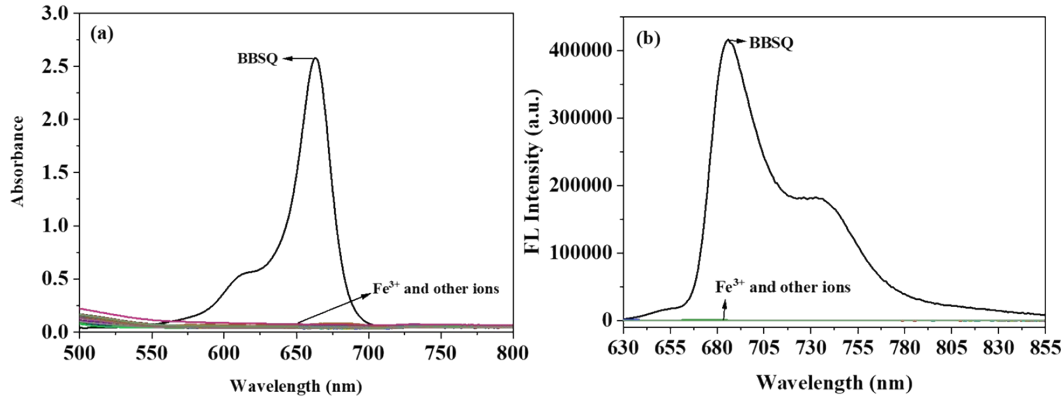

Figure S9 (a) UV-vis absorption spectra and (b) fluorescence emission spectra of BBSQ (10 μM) in presence of Fe^{3+} (20 equiv.) along with other metal ions (20 equiv.).

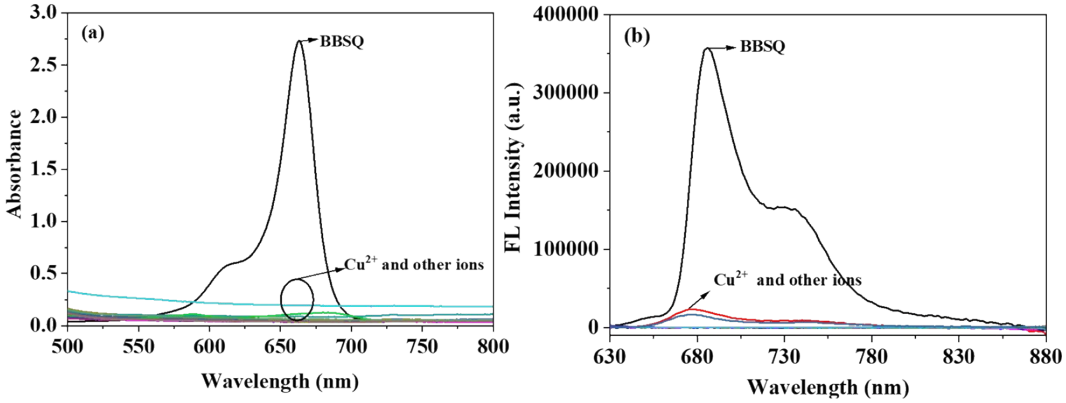

Figure S10 (a) UV-vis absorption spectra and (b) fluorescence emission spectra of BBSQ (10 μM) in presence of Cu^{2+} (20 equiv.) along with other metal ions (20 equiv.).

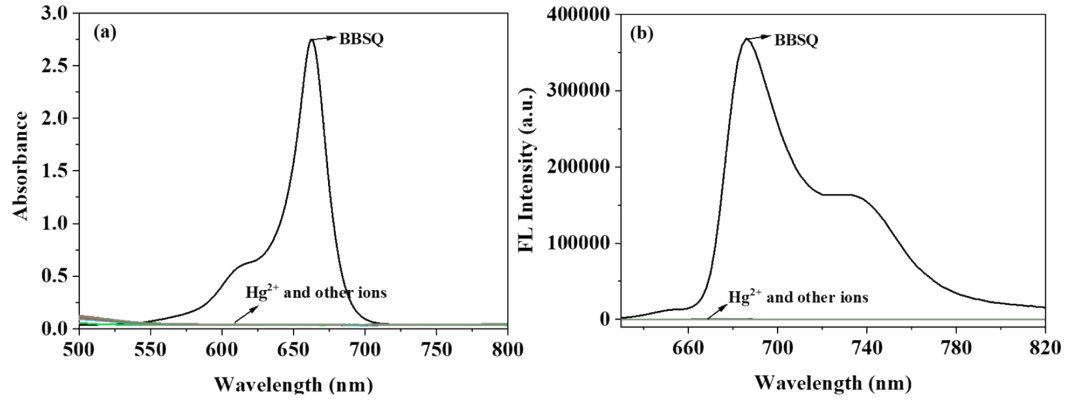

Figure S11 (a) UV-vis absorption spectra and (b) fluorescence emission spectra of BBSQ (10 μM) in presence of Hg^{2+} (20 equiv.) along with other metal ions (20 equiv.).

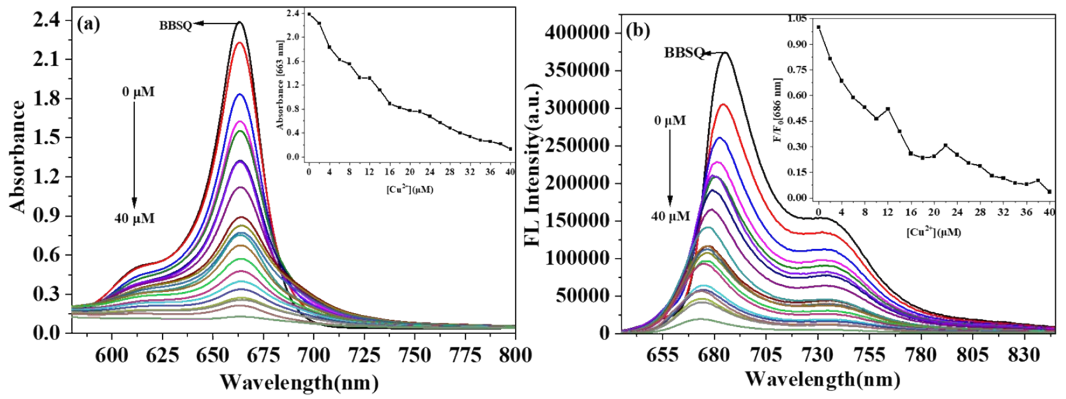

Figure S12 (a) UV-vis absorption and (b) fluorescence spectral titrations of BBSQ acetonitrile solution (10 μM) with Cu^{2+} (0-40 μM); inset: the concentration titration curves of absorbance at 663 nm (a) and fluorescence emission intensity at 686 nm (b) with increasing Cu^{2+} concentration.

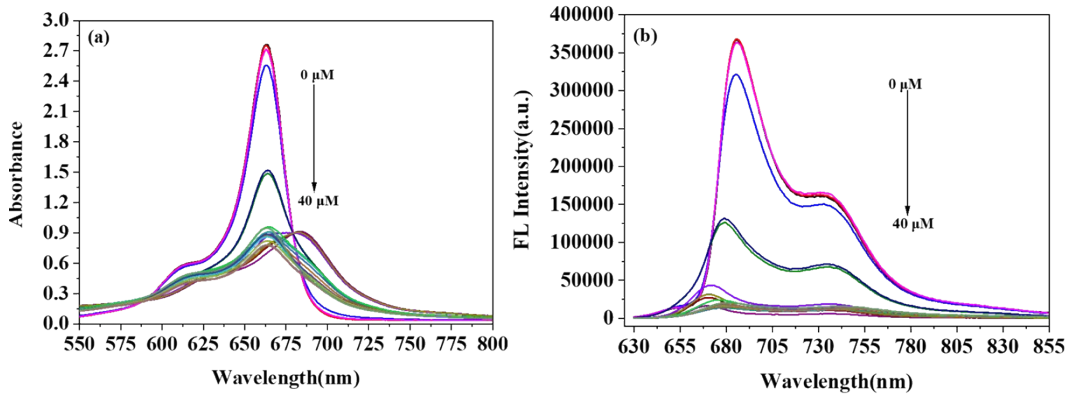

Figure S13 (a) UV-vis absorption and (b) fluorescence spectral titrations of BBSQ acetonitrile solution (10 μM) with Hg^{2+} (0-40 μM).

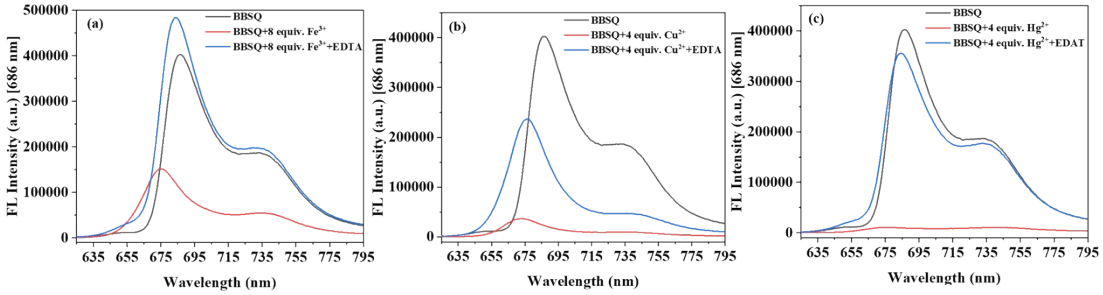

Figure S14 Fluorescence emission spectra of BBSQ and BBSQ in response to (a) Fe^{3+}, (b) Cu^{2+} and (c) Hg^{2+} ions with/ without adding EDTA.

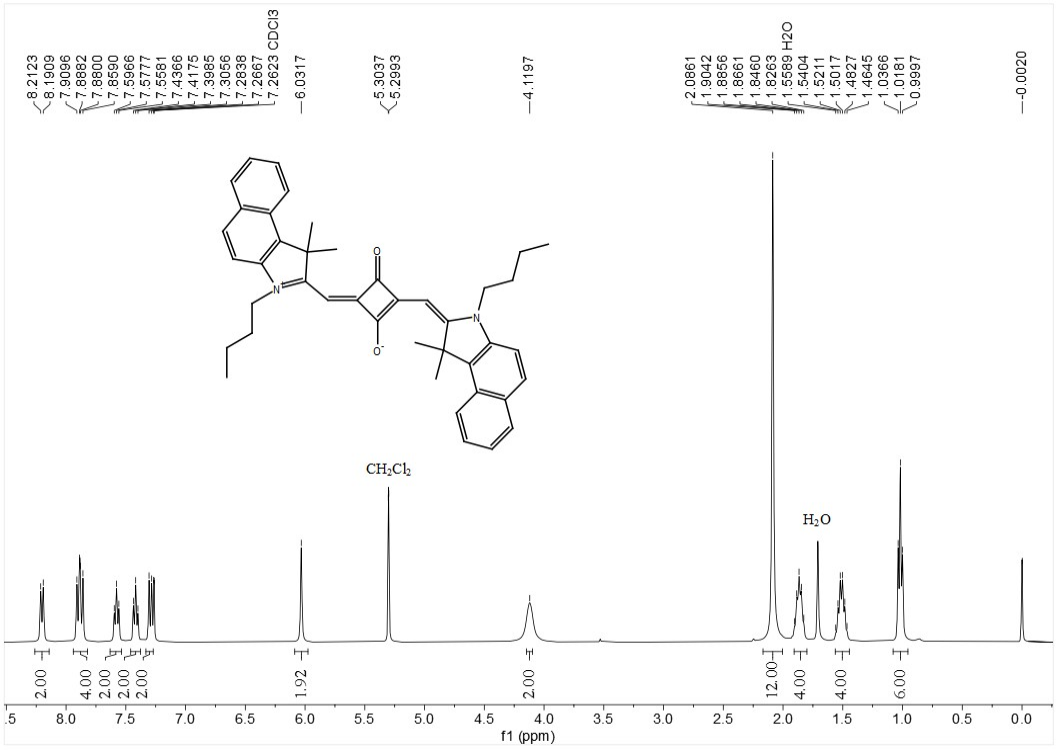

Figure S15 ^{1}H NMR spectrum (400 MHz, $CDCl_3$) of BBSQ.

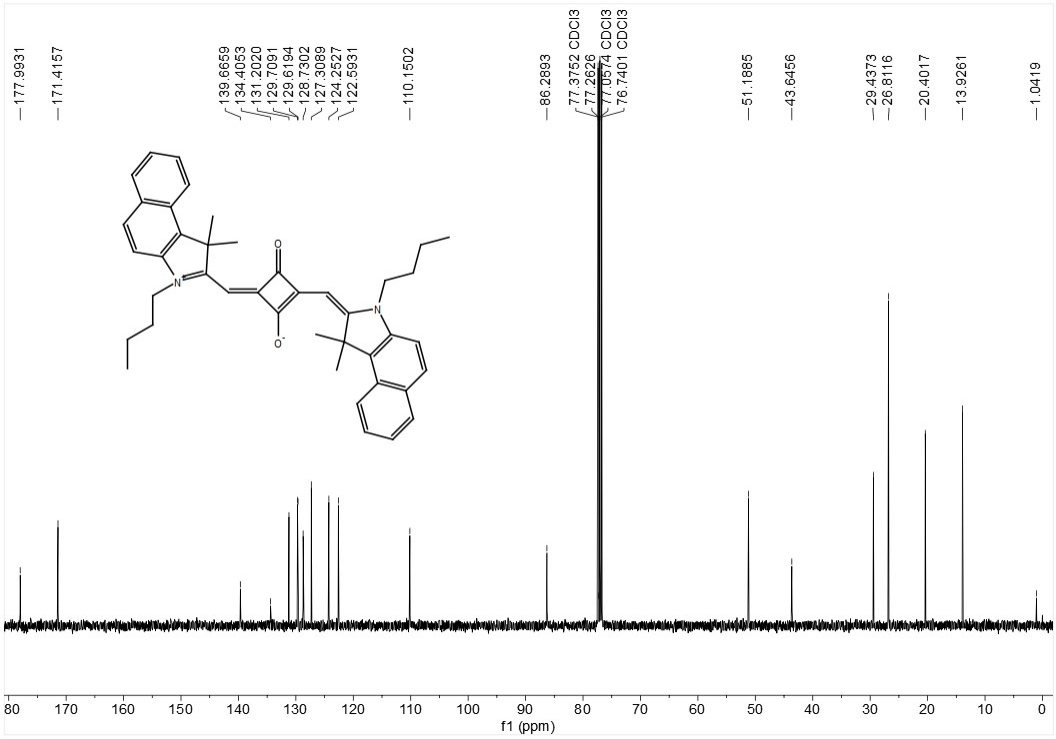

Figure S16 ^{13}C NMR spectrum (101 MHz, $CDCl_3$) of BBSQ.

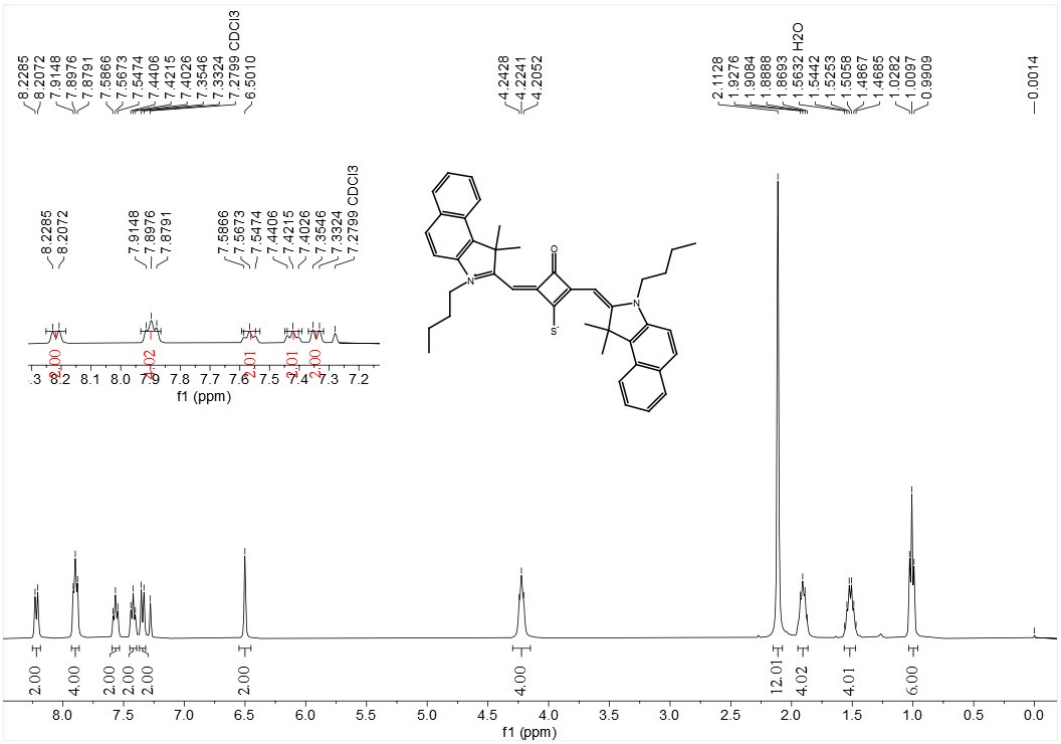

Figure S17 ^{1}H NMR spectrum (400 MHz, $CDCl_3$) of BBSQ-S.

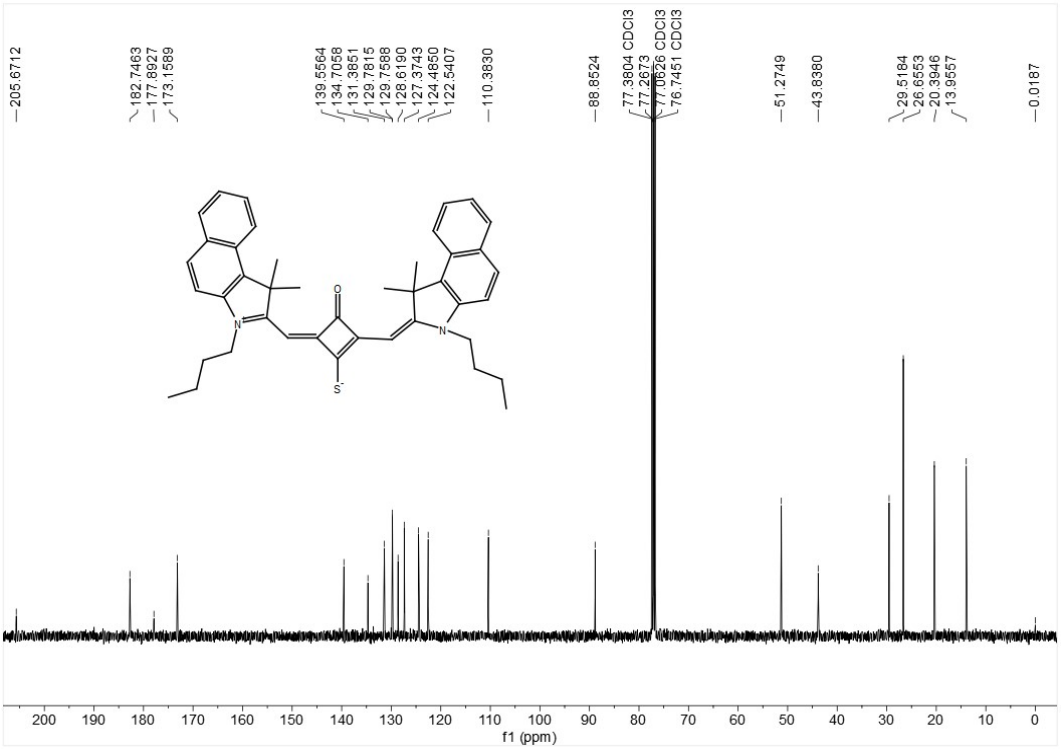

Figure S18 ^{13}C NMR spectrum (101 MHz, $CDCl_3$) of BBSQ-S.

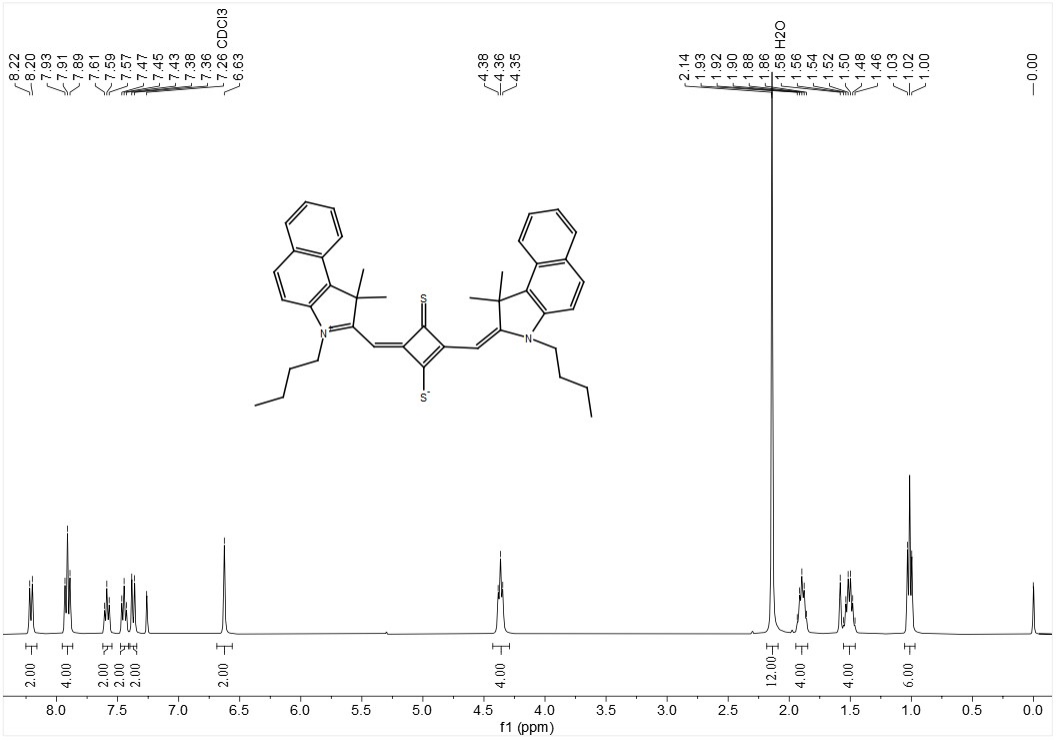

Figure S19 ^{1}H NMR spectrum (400 MHz, $CDCl_3$) of BBSQ-SS.

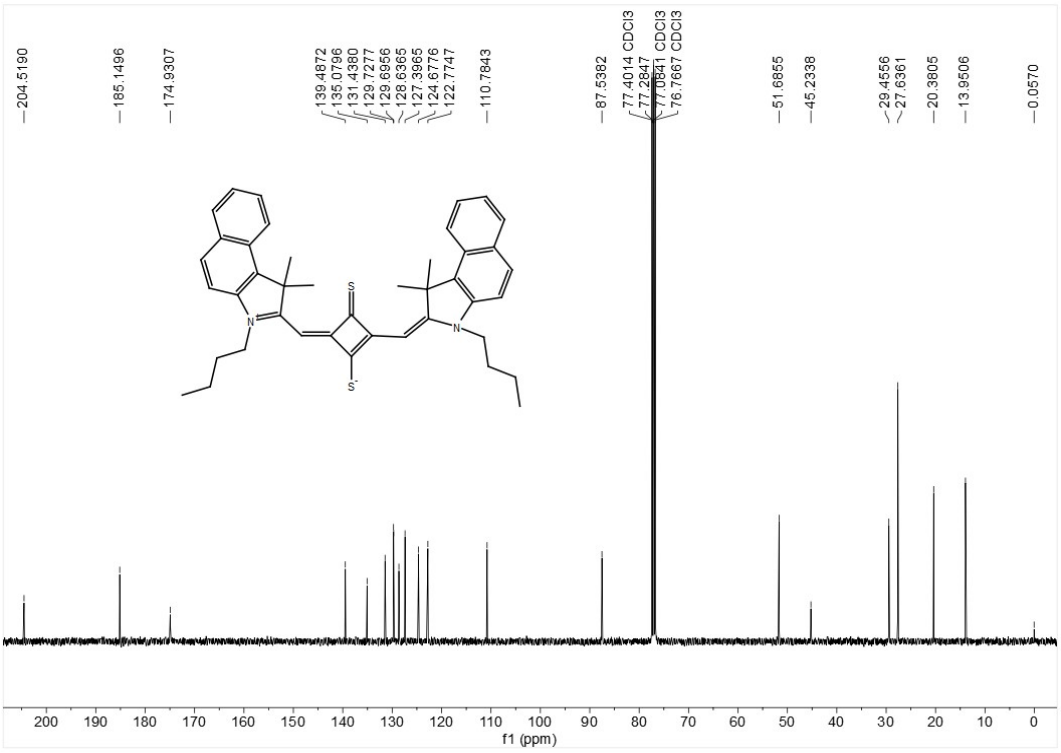

Figure S20 ^{13}C NMR spectrum (101 MHz, $CDCl_3$) of BBSQ-SS.

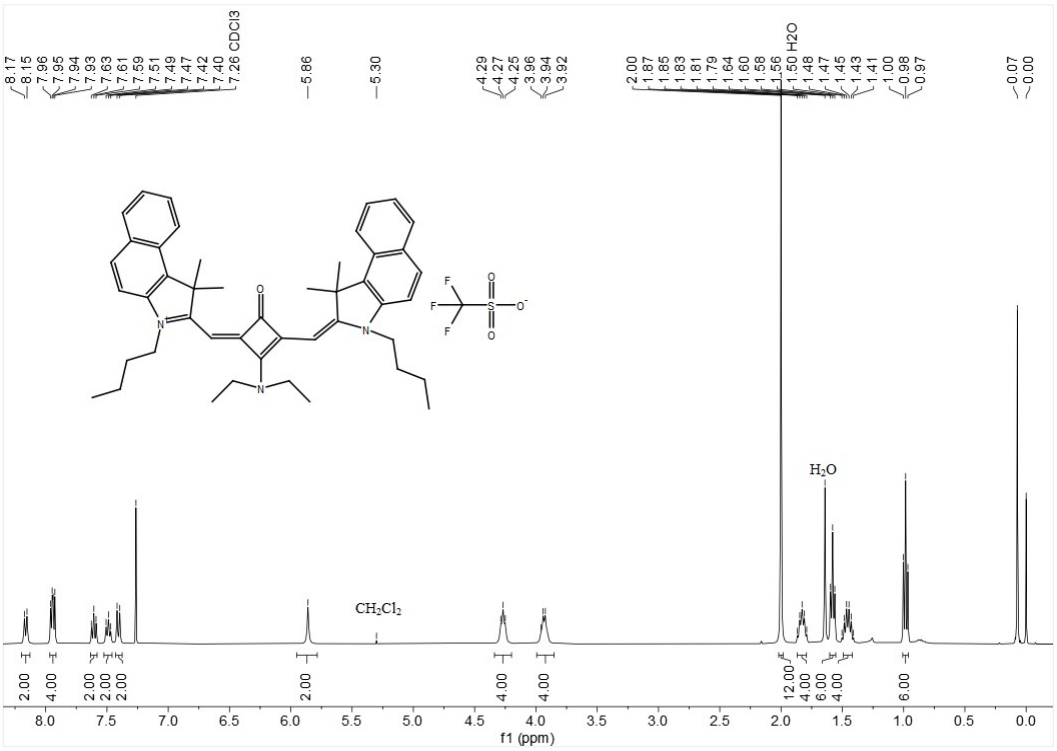

Figure S21 ^{1}H NMR spectrum (400 MHz, $CDCl_3$) of BBSQ-NEt.

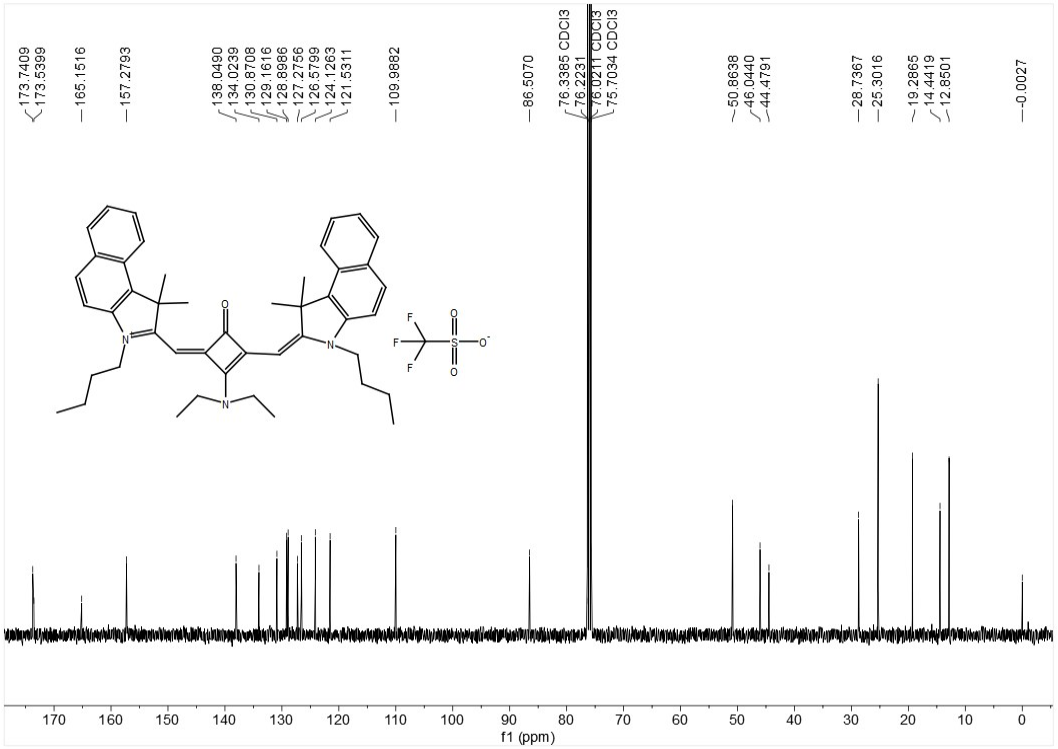

Figure S22 ^{13}C NMR spectrum (101 MHz, $CDCl_3$) of BBSQ-NEt.

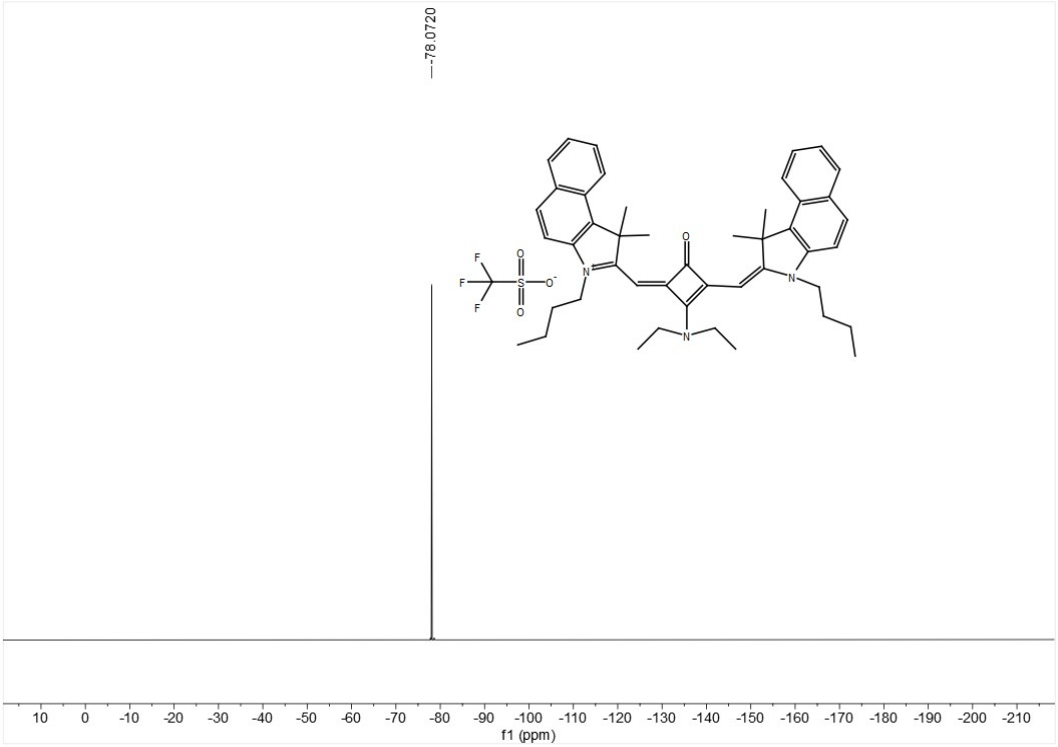

Figure S23 ^{19}F NMR spectrum (376 MHz, $CDCl_3$) of BBSQ-NEt.

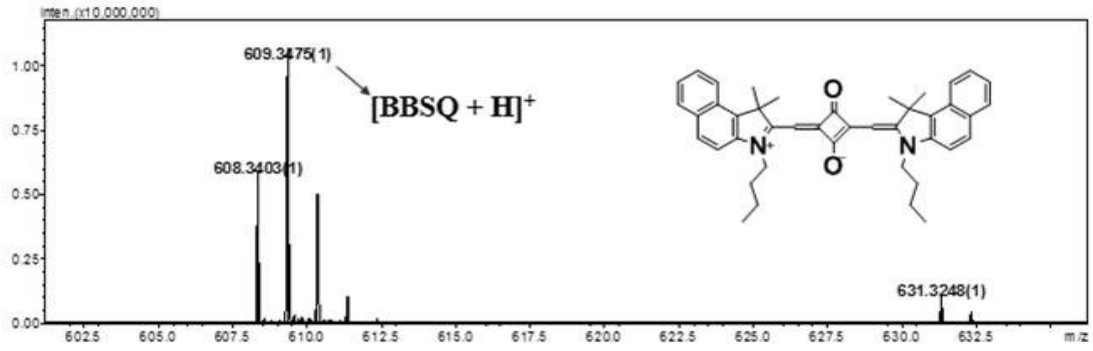

Figure S24 HRMS (ESI) of $[BBSQ+H]^+$: 609.3475.

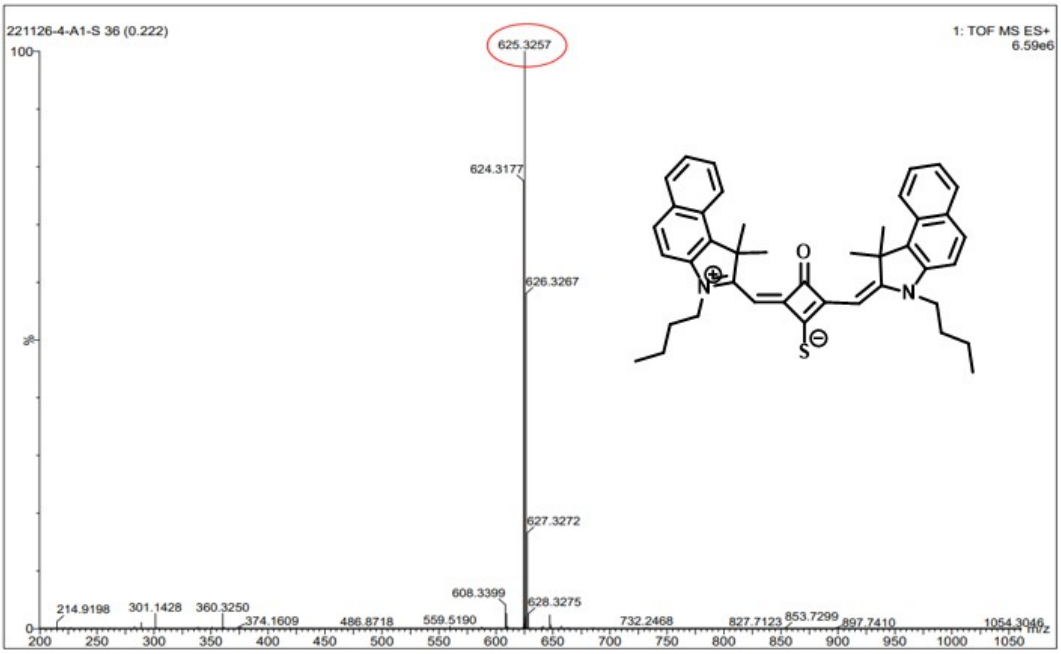

Figure S25 HRMS (ESI) of $[BBSQ-S+H]^+$: 625.3257.

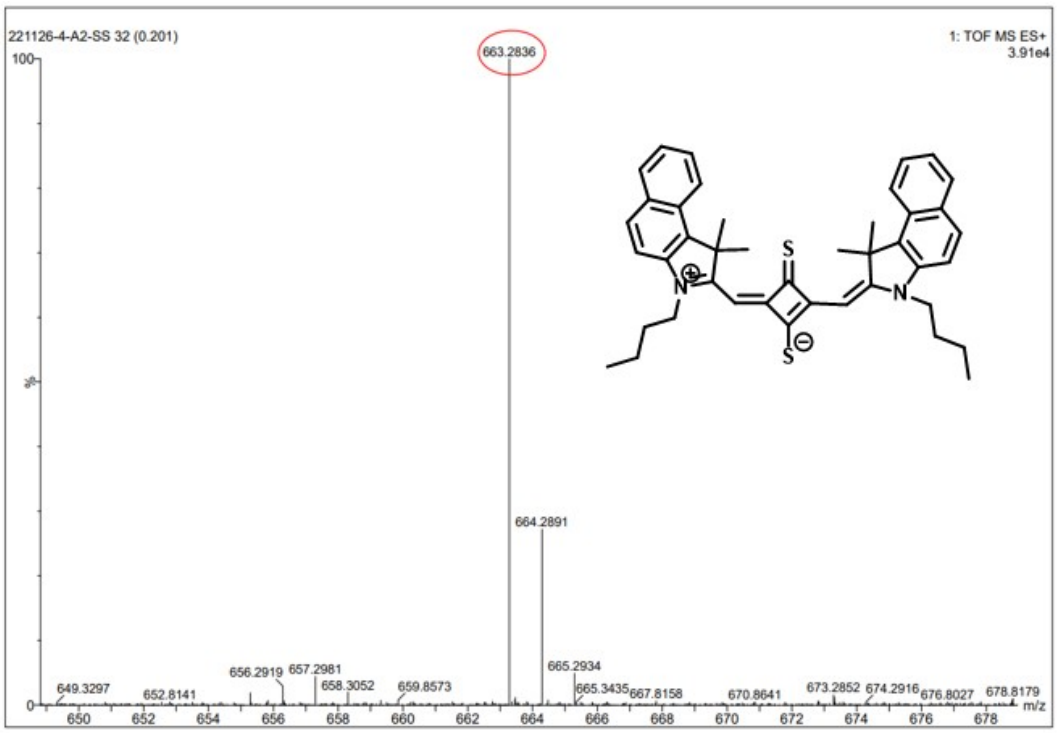

Figure S26 HRMS (ESI) of $[BBSQ\text{-}SS+Na]^+$: 663.2836.

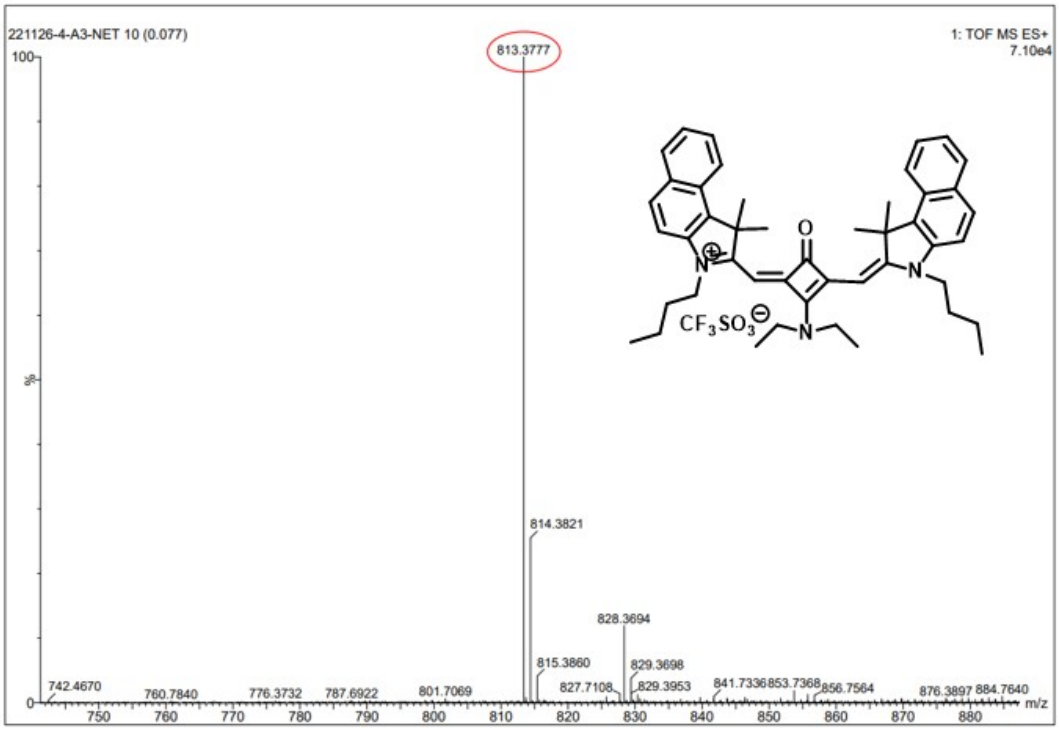

Figure S27 HRMS (ESI) of $[BBSQ\text{-}NEt]^+$: 813.3777.

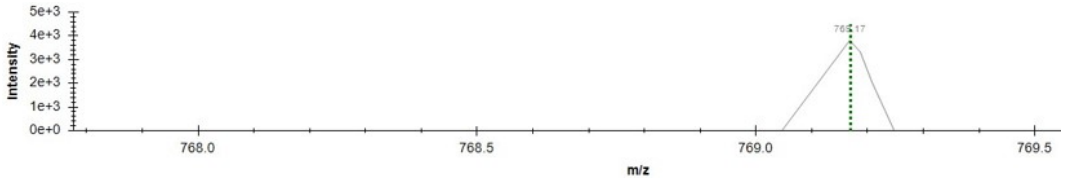

Figure S28 HRMS (ESI) of [BBSQ-$FeCl_3^+$]: 769.17.

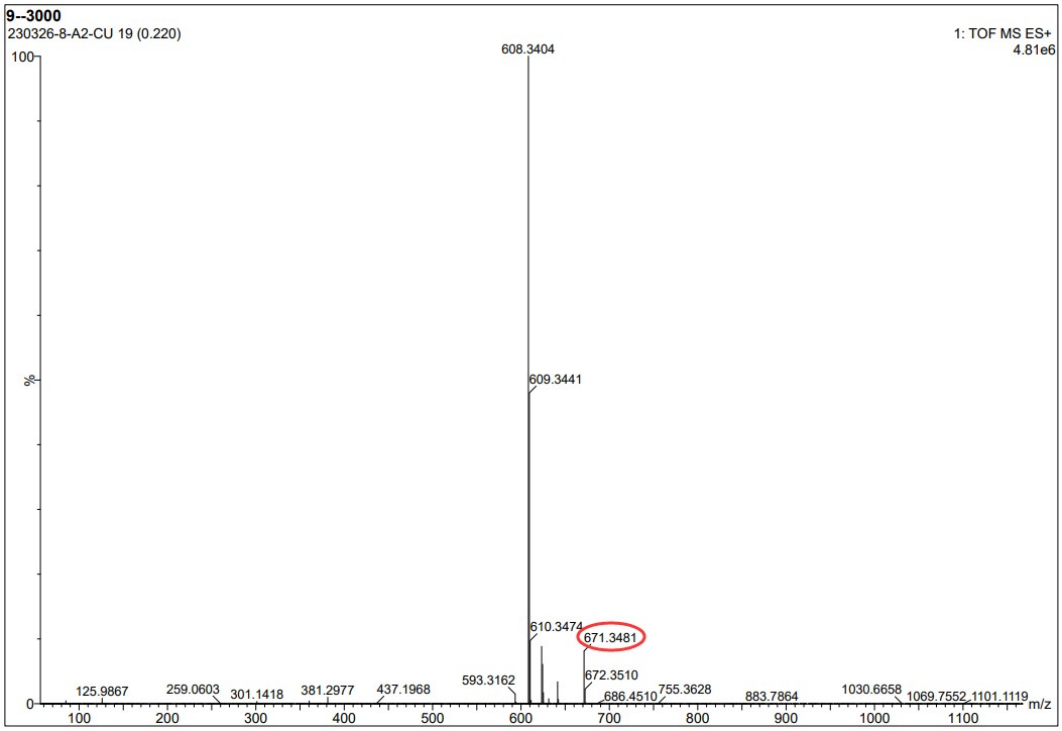

Figure S29 HRMS (ESI) of [BBSQ-Cu^{2+}]: 671.3481.

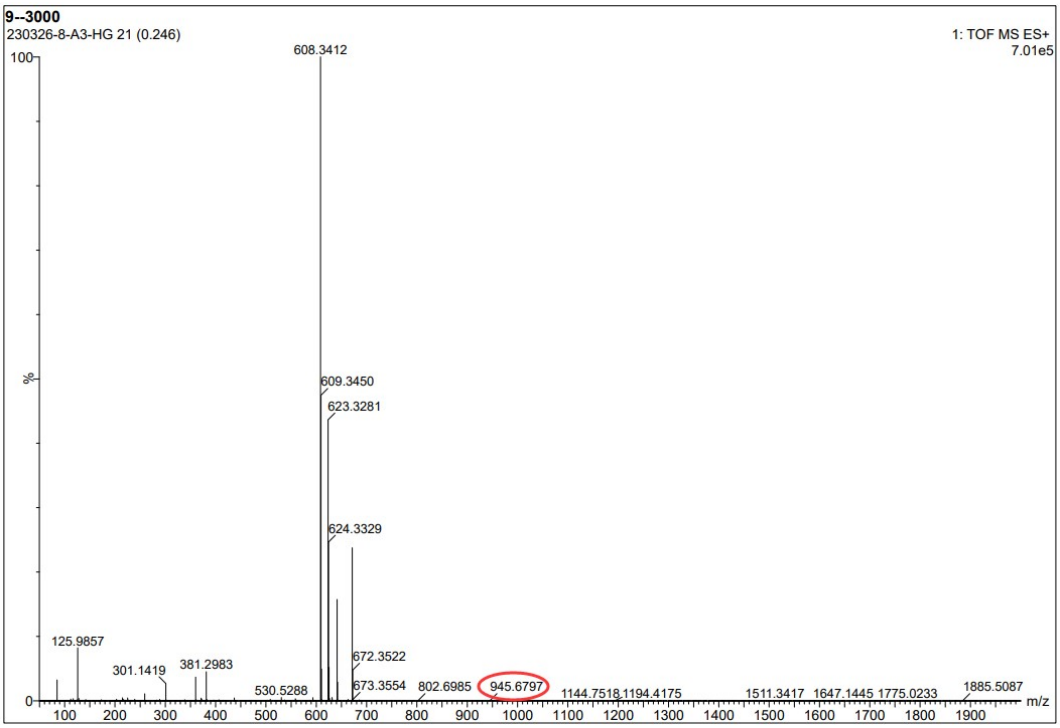

Figure S30 HRMS (ESI) of [BBSQ-Hg^{2+}+2CH_3CN+2H_2O+OH^-]: 945.6797.

References

1. F. Yan, T. Zheng, D. Shi, Y. Zou, Y. Wang, M. Fu, L. Chen and W. Fu, *Sens Actuators B Chem*, 2015, **215**, 598-606.
2. H.-T. Tsai, Y. R. Bhorge, A. J. Pape, S. N. Janaki and Y.-P. Yen, *J Chin Chem Soc*, 2015, **62**, 316-320.
3. J. Liu and Y. Qian, *J Lumin*, 2017, **187**, 33-39.
4. L. Wang, H. Li and D. Cao, *Sens Actuators B Chem*, 2013, **181**, 749-755.
5. A. Singh, S. Sinha, R. Kaur, N. Kaur and N. Singh, *Sens Actuators B Chem*, 2014, **204**, 617-621.
6. Y. K. Jang, U. C. Nam, H. L. Kwon, I. H. Hwang and C. Kim, *Dyes Pigm*, 2013, **99**, 6-13.
7. H. Zhang, L. Feng, Y. Jiang, Y. T. Wong, Y. He, G. Zheng, J. He, Y. Tan, H. Sun and D. Ho, *Biosens Bioelectron*, 2017, **94**, 24-29.
8. X.-X. Hu, X.-L. Zheng, X.-X. Fan, Y.-T. Su, X.-Q. Zhan and H. Zheng, *Sens Actuators B Chem*, 2016, **227**, 191-197.
9. R. An, D. Zhang, Y. Chen and Y.-z. Cui, *Sens. Actuators B Chem*, 2016, **222**, 48-54.
10. M. Yang, H. Wang, J. Huang, M. Fang, B. Mei, H. Zhou, J. Wu and Y. Tian, *Sens Actuators B Chem*, 2014, **204**, 710-715.

11. Y. Liu, E.-B. Yang, R. Han, D. Zhang, Y. Ye and Y.-F. Zhao, *Chin Chem Lett*, 2014, **25**, 1065-1068.

12. Y. Gao, C. Zhang, S. Peng and H. Chen, *Sens. Actuators B Chem*, 2017, **238**, 455-461.

13. M. Ozdemir, *Sens. Actuators B Chem*, 2017, **249**, 217-228.

14. Y. Wang, F. Pan, Y. Zhang, F. Peng, Z. Huang, W. Zhang and W. Zhao, *Analyst*, 2016, **141**, 4789-4795.